Petroleum Science 19 (2022) 2932–2940

Contents lists available at ScienceDirect

Petroleum Science

journal homepage: www.keaipublishing.com/en/journals/petroleum-science

Original Paper

Pore scale performance evaluation and impact factors in nitrogen huff-n-puff EOR for tight oil

Yi-Lei Song, Zhao-Jie Song*, Yun-Fei Zhang, Ze-Hui Xie, Li-Chao Zhang, Dai-Gang Wang, Gang Hui

College of Carbon Neutral Energy, State Key Laboratory of Petroleum Resources and Prospecting and Unconventional Petroleum Research Institute, China University of Petroleum-Beijing, Beijing, 102249, China

A R T I C L E I N F O

Article history:
Received 22 March 2022
Received in revised form
19 May 2022
Accepted 19 May 2022
Available online 25 May 2022

Edited by Yan-Hua Sun

Keywords:
Tight oil reservoirs
N_2 huff-n-puff
Pore-level production characteristics
Impact factors
Nuclear magnetic resonance

A B S T R A C T

Nitrogen huff-n-puff (N_2 HnP) appears to be an economical and high-efficiency enhanced oil recovery (EOR) technique for tight oil reservoirs. There is however a lack of understanding of the pore-level EOR performance of N_2 HnP under tight reservoir conditions. In this work, a non-magnetic reactor was created and combined with a nuclear magnetic resonance (NMR) device for real-time monitoring of oil distribution in the HnP experiment. N_2 HnP experiments were then performed in a tight sandstone core sample at a temperature of 353 K and an injection pressure $\geq$ 24 MPa. The pore-level oil distribution under reservoir conditions was monitored and the EOR performance of N_2 HnP in specific pores was analyzed. The pore throat structures of the core sample and the phase behavior of the N_2-oil system were analyzed to elucidate the EOR mechanism of N_2 HnP. An oil recovery factor of 37.52% can be achieved after four cycles, which proves the EOR potential of N_2 HnP for tight reservoirs. The highest recoveries after N_2 HnP are obtained in the large pores, followed by the medium pores, the small pores, and finally the micro pores. Increases in soaking time and injection pressure resulted in slight and pronounced increases in oil recovery, respectively, both of which are mainly reflected in the first cycle. Specifically, increasing the soaking time only slightly improves the cumulative oil recovery in the small pores while increasing the injection pressure significantly improves the cumulative oil recovery in the small, medium, and large pores simultaneously. However, variations in both injection pressure and soaking time have a negligible effect on the cumulative oil recovery of the micro pores.

1. Introduction

The exploration and development of unconventional energy, especially tight oil, has been stepped up worldwide (Feng et al., 2020). Tight oil reservoirs are dominated by nano-scale pores, which leads to extremely low permeability and high flow resistance such as capillary force (Yu et al., 2015). Although technologies such as horizontal wells have been developed, the recovery factor of tight oil reservoirs is still not high (Song et al., 2020). An effective EOR technology is needed to improve the ultimate tight oil recovery (Dong et al., 2020a; Wang et al., 2018).

Recently, gas huff-n-puff (HnP) to improve tight oil recovery has attracted widespread attention from scientists and engineers (Burrows et al., 2020; Jia et al., 2016). The gas HnP method mainly includes three main parts, namely the huff process, the soaking process, and the puff process (Wan et al., 2018; Zhu et al., 2020). The gases commonly used in the process of gas injection are CO_2 and N_2. CO_2 is characterized by lower minimum miscible pressure and higher sweep efficiency (Song et al., 2021a). However, it is not convenient to use CO_2 in some cases due to the limited gas source and strong corrosiveness. N_2 is considered a cost-effective, non-corrosive, and economic option for gas HnP research (Lu et al., 2017; Yue et al., 2018).

Lots of scholars have studied the performance of gas HnP in unconventional formations using numerical simulation (Wan and Liu, 2018). Sheng et al. (2016) compared the EOR performance of CH_4, CO_2, and N_2 HnP in the Middle Bakken formation based on the Computer Modeling Group (CMG). Zhang et al. (2018) proposed a modified numerical model to investigate the CO_2 HnP in a tight oil

* Corresponding author.
E-mail address: songz@cup.edu.cn (Z.-J. Song).

https://doi.org/10.1016/j.petsci.2022.05.012
1995-8226/

reservoir. The effects of phase behavior change and molecular diffusion were considered in their model. Zuloaga et al. (2017) compared the production performance of CO_2 HnP and CO_2 flooding in the Bakken reservoir using a numerical compositional model with multiple hydraulic fractures. Hamdi et al. (2018) evaluated the lean and rich HnP in the Duvernay shale reservoir based on a compositional numerical model. They found that the optimized HnP has doubled the recovery factor compared to depletion development in 20 years. Sun et al. (2019) proposed a numerical model based on the CMG to analyze the CO_2 HnP. Obviously, many valuable insights have been gained through numerical simulation research in terms of enhanced tight oil recovery by gas HnP. However, unconventional reservoirs differ greatly from conventional reservoirs, with various scales of fractures and significant nanopore confinement effects. The accuracy of the current numerical simulation results for unconventional reservoirs is doubtful, and the conclusions of many simulations need to be verified through indoor experiments.

The core scale experiment has always been regarded as the most direct method to study the EOR performance of gas HnP in tight or shale formations (Li et al., 2020). However, it is difficult to conduct experimental studies due to the high cost of equipment and time (Nguyen et al., 2018; Mahzari et al., 2021). Some researchers have carried out the gas HnP experiment with pore-scale using the weighing method. Yu et al. (2017) evaluated the production performance of N_2 continuous injection and N_2 HnP in tight core samples by recording weight changes at different development stages. Li et al. (2018) studied the potential for extracting hydrocarbons of CO_2 HnP in Eagle Ford cores. They found that the weight of the saturated oil core dropped from 128.16 g to 126.52 g after seven HnP cycles, and the corresponding oil recovery factor was 67.97%. Zhu et al. (2020) investigated the recovery factors of CO_2 HnP in tight cores with fractures under different injection pressures and injection times by recording mass changes. Altawati et al. (2021) conducted a cryogenic N_2 HnP experiment and found that the liquid N_2 HnP technology can increase the tight oil recovery factor to 78%, and increasing the injection pressure can further increase the recovery factor. Based on the weighing method, the huge potential of gas HnP to enhance the tight oil recovery has been confirmed. However, the weighing method presents many shortcomings, such as large measurement error due to the big gap between the quality of the produced oil and the core; the pressure must be reduced to atmospheric pressure in the huff stage; only the change in oil recovery can be measured, and the remaining oil distribution cannot be observed.

Nuclear magnetic resonance (NMR) technology can be used to analyze the pore structure and fluid distribution characteristics by measuring the magnitude of transverse relaxation time (T_2). To make up for the limitation of the weighing method, some recent studies have focused on the application of NMR in gas injection experiments (Huang et al., 2019; Dong et al., 2020a,b; Qian et al., 2018). The changes in the NMR T_2 time curves before and after gas HnP could be analyzed to study the flow of movable fluids and the distribution of remaining oil. Wan et al. (2018) carried out gas HnP and waterflooding experiments to elucidate the EOR performance in Xinjiang tight formations using the low-field NMR. The results showed that oil production mainly occurred in the first few cycles and in specific pores. Ma et al. (2019) studied the effect of cycle numbers and production pressure on the effectiveness of CO_2 HnP with the NMR technique. They found that macropores contribute more to oil recovery compared to small ones. Bai et al. (2019) performed CO_2 HnP experiments with the NMR technique in a tight core plug with artificial fractures to investigate the effects of fractures on remaining oil distribution. The study found a 14% increase in the ultimate recovery factor of the fractured core compared to the fractured-free core. Du et al. (2020) compared the CO_2 HnP and flooding in a tight reservoir. NMR T_2 spectra and one-dimensional NMR signal distributions were used to observe the variation of oil saturation. In Wei et al. (2020)' study, the mass change between the matrix and fracture at different stages during CO_2 HnP was under surveillance by NMR technology. NMR T_2 spectra and 2D longitudinal images of the core sample during the experiments were recorded to understand the oil recovery dynamics in their study.

Due to the limitations of NMR equipment, most of the current studies have been conducted under mild conditions. The NMR signal is often measured at atmospheric pressure and room temperature, which leads to errors in the measurement results. In fact, online NMR devices have been previously developed that can measure signals at high temperatures and pressures in real-time (Song et al., 2022b). However, it is not suitable for HnP experimental studies due to operational difficulties and lower data accuracy. Therefore, new devices or methods need to be proposed to accurately detect the NMR signal in HnP experiments. In addition, few experimental studies have been conducted to investigate the EOR capabilities of N_2 HnP under tight oil reservoir conditions. It is necessary to further clarify the EOR feasibility and mechanism of N_2 HnP.

In this study, a non-magnetic reactor for HnP experiments was developed and N_2 HnP experiments were then performed on a tight core sample. NMR T_2 spectra and spatial distribution of 1D NMR signals under reservoir conditions were recorded to observe the variation in oil distribution. The pore throat structures of the core sample and the phase behavior of the N_2-oil system were analyzed to elucidate the EOR mechanism of N_2 HnP. The EOR potential and feasibility of N_2 HnP were discussed, specifically, the EOR performances of N_2 HnP in specific pores were analyzed at different cycle numbers, soaking times, and injection pressures.

2. Experimental

2.1. Materials

A dead oil sample and a sandstone core plug were collected from a target area with a depth from 1639.1 to 1696.2 m in northeastern China. The viscosity and density of the oil sample at a temperature of 353 K and a pressure of 0.101 MPa were 3.15 mPa s and 815 kg/m^3, respectively. The molar composition of the deal oil sample was measured and the results were presented in Section 3.2. The diameter, length, porosity and permeability of the tight core plug were 2.5 cm, 6.06 cm, 9.3442% and 0.0356 mD, respectively. To accurately measure the oil signal, deuteroxide (D_2O) was used to saturate the core samples. The purity of N_2 gas used in this work was 99.99%.

2.2. Apparatus

Fig. 1 presents the schematic outline of the N_2 HnP device. The experimental setup consists mainly of an injection system, a production system, and an NMR measurement system. D_2O, oil and N_2 are stored in separate containers and will be pumped into the coreholder or non-magnetic reactor through a syringe pump. The coreholder is used for fluid initialization rather than gas HnP experiments. This non-magnetic reactor is specially made for HnP experiments, with a maximum temperature resistance of 393.15 K and pressure resistance of 40 MPa. The core sample in the reactor can be scanned in any direction using a low-field NMR system to measure the NMR signal. In the production system, a back-pressure regulator is employed to control the outlet pressure.

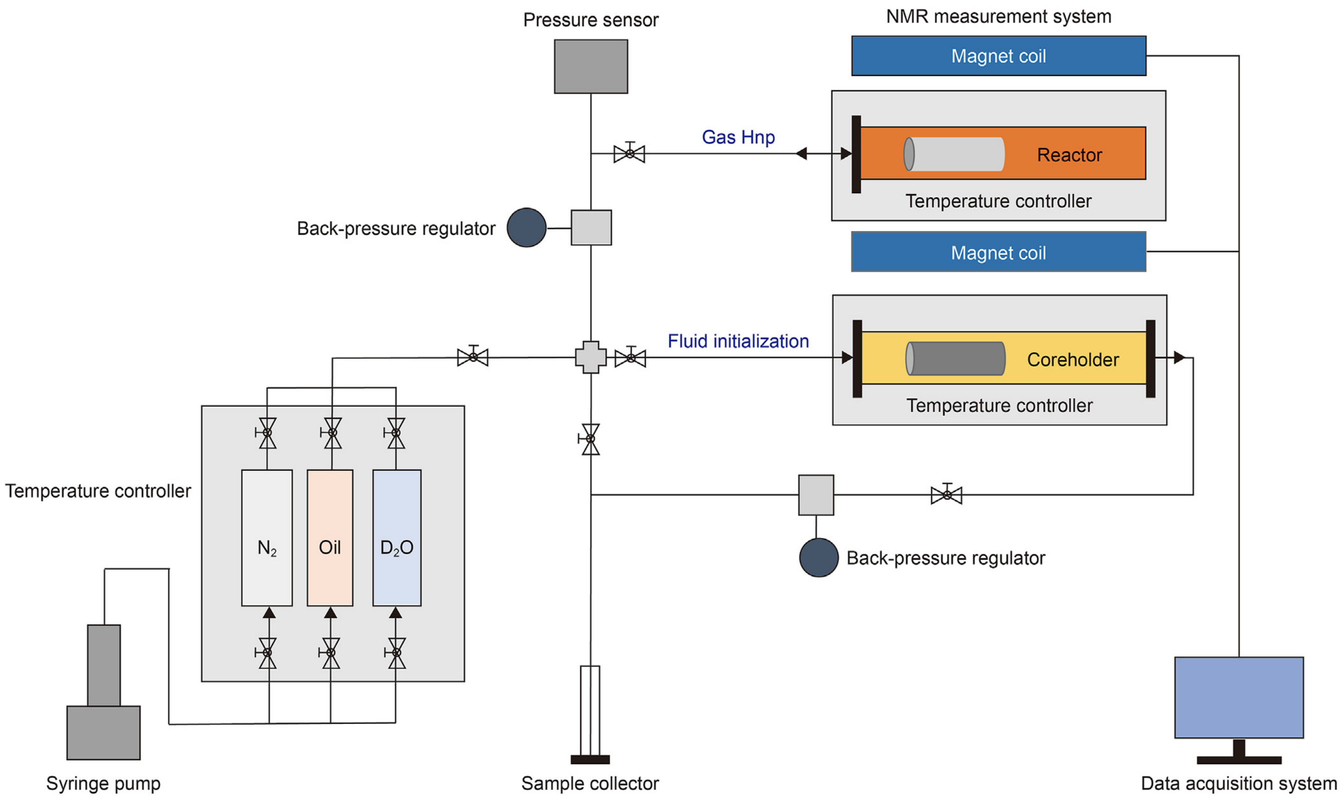

Fig. 1. Schematic diagram of the N_2 HnP device.

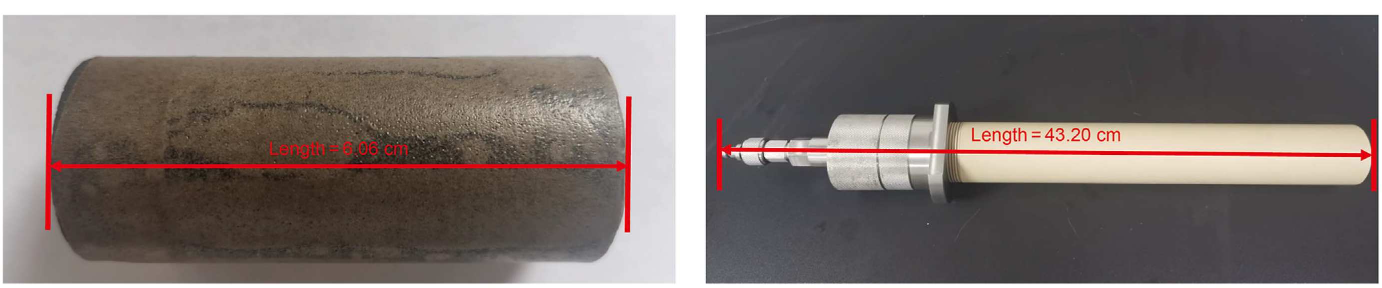

(a) (b)

Fig. 2. Diagram of the core plug (**a**) and non-magnetic reactor (**b**).

2.3. Procedures

(1) Sample preparation. The core plug was cleaned with petroleum ether for 21 days. Then, the core sample was dried for 2 days, followed by the permeability, porosity, and pore size distribution (PSD) measurements.
(2) Fluid initialization. The core sample was dried for 2 days and then placed into the coreholder to saturate the D_2O at an injection pressure of 20 MPa. Next, the oil was injected into the core at the same injection pressure of 20 MPa until the produced fluid no longer contained water. After that, the outlet pressure was conditioned to 20 MPa, and the oil was still pumped into the core plug until the system pressure reaches 20 MPa for 2 days.
(3) HnP. The side of the oil-saturated core was wrapped with heat-shrinkable film and placed in the reactor as shown in Fig. 2. N_2 was then injected into the reactor, and the injection was stopped when the pressure rose to a pre-specified value. In this case, the core was surrounded by N_2, and thus the confining pressure was the same as the pressure at the ends of the core. After soaking for a pre-specified time, puff production was carried out at a back pressure of 15 MPa and continued for 12 h.
(4) Change the experimental conditions and repeat the Steps (1)–(3).

During the experiment, the system temperature was set to 353 K, and the NMR signals were recorded at set intervals. The amplitude and relaxation rate of the NMR relaxation signal of fluids in porous media were measured, and the collected signals were mathematically converted into the T_2 spectrum. The NMR T_2 spectrum shows the percentage of different relaxation times. The T_2 value is in proportion to the pore radius of the rock, i.e., larger pores in the core present longer relaxation times. Therefore, the NMR T_2 spectra could provide a direct reflection of the fluid distribution in pores of different sizes.

3. Results and discussion

Three N_2 HnP experiments are conducted at different soaking times and injection pressures to examine the feasibility and governing factors of N_2 HnP. For comparability, the same core sample is used for all experiments. The basic parameters for each test group are given in Table 1.

3.1. Pore throat size distribution

The pore throat structure of tight reservoirs is difficult to be described and the pore throat size distribution needs to be characterized using a combination of different techniques. In this section, the NMR signals of the core samples saturated with deionized water are measured and combined with mercury-injection capillary pressure data to reveal the pore size distribution of the core sample. Fig. 3 shows a comparison between the pore size distribution measured by NMR and mercury intrusion. They are in good agreement in terms of morphology and magnitude. Because the mercury intrusion cannot accurately characterize micro and small pore distributions, the pore size distributions are poorly matched in the pore radius (r) less than 0.2 μm. Overall, the pore radius of this core plug is mainly in the range of 0.004–1.000 μm, with a peak at 0.250 μm.

Subsequently, the dynamic changes of T_2 spectra during N_2 HnP are used to analyze pore throat structure of the core sample. The T_2 spectra under different stages during tests 1, 2 and 3 are given in Fig. 4. The T_2 spectra can be divided into two parts, small T_2 region (T_2 < 4.55 ms, approximately corresponding to r < 0.022 μm) and large T_2 region (T_2 > 4.55 ms, approximately corresponding to r > 0.022 μm). The signal in the large T_2 region is consistently decreasing with increasing cycles. However, the signal in the small T_2 region is not continuously decreasing with increasing cycles, and sometimes even increases. This could mean that the small T_2 region is primarily flow channels (throats), while the large T_2 region is primarily oil storage spaces (pores). There are two important reasons to support the above conclusion. First, the T_2 value is in proportion to the pore throat radius of the rock, and scholars generally refer to the narrow space between two open pores as the throat (Kewen and Ning, 2008; Chen et al., 2019; Huang et al., 2020). Second, some researchers have found that the pore-to-throat size ratio of tight reservoirs in this area tends to be in the range of 50–600 (Xiao et al., 2017), which supports our analysis. Therefore, the small T_2 region and large T_2 region may correspond to the throat-majority region and pore-majority region, respectively. It should be noted that the throat-majority region still contains pores and the pore-majority region still contains throats. In addition, there is no essential difference between throats and pores. To analyze the variation of the remaining oil in pores of different radii, the pore space is uniformly subdivided into four parts according to the pore size and amount of saturated oil: micro pores (4.55–24.09 ms, approximately corresponding to 0.022–0.115 μm), small pores (24.09–55.43 ms, approximately corresponding to 0.115–0.264 μm), medium pores (55.43–116.23 ms, approximately corresponding to 0.264–0.554 μm), and large pores (> 116.23 ms, approximately corresponding to > 0.554 μm). The initial oil volume in each pore part is equal.

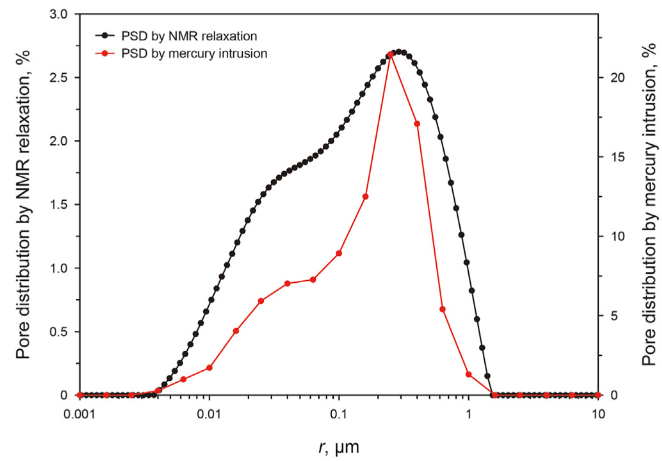

Fig. 3. Pore size distribution measured by NMR relaxation and mercury intrusion.

3.2. Phase behavior of N_2-oil system

The molar composition of the deal oil sample is measured using gas chromatography, the result is shown in Table 2. Then, the phase behavior of the N_2-oil system is simulated using the two-phase flash model developed by Song et al. (2021b, 2022a). To improve the accuracy of the calculations, the model for flash calculation is optimized using the viscosity and density data of the oil sample at 353 K and 0.101 MPa. The molar compositions and properties of the oil phase and gas phase after N_2 injection at 24 and 28 MPa, respectively, are calculated as shown in Table 2. The amount of injected N_2 is sufficient, accounting for 2/3 of the total moles. The result shows that a large amount of N_2 can dissolve in the oil phase and reduce its density, but it has no significant effect on the viscosity of the oil phase. As the pressure increases, the solubility of N_2 increases. In addition, lighter components of the oil such as pentane, hexane and heptane enter the gas phase. In the puff state, these substances will be released along with the nitrogen as the pressure drops, resulting in an increase in the molecular weight of the remaining oil. This could explain why the T_2 spectral curve is shifted to the left after the N_2 HnP. As shown in Fig. 4, the amplitude of T_2 drops to zero in the range of 300–450 ms, making the T_2 spectral curve appear to be shifted to the left. This is since the T_2 value is not only related to the pore size but also to the properties of the fluid. The lighter components in the oil are extracted at the end of the N_2 HnP, causing the remaining oil to become heavier and the T_2 spectrum to shift to the left by a small amount. In this case, the conversion factor between the T_2 value and the pore size changes slightly. However, we could still use the T_2 spectrum to analyze the remaining oil distribution as the experiments are conducted with dead oil and the extraction effect is not obvious. If there are many light components in the oil sample and the extraction effect is strong, the T_2 spectrum may need to be corrected before it can be employed.

3.3. EOR capability

The overall NMR signal is in proportion to the oil quality in the

Table 1
Basic parameters of N_2 HnP.

Test	Injection pressure, MPa	Soaking time, h	Temperature, K	Back pressure, MPa	Total cycle
1	24	12	353	15	4
2	24	24	353	15	4
3	28	12	353	15	4

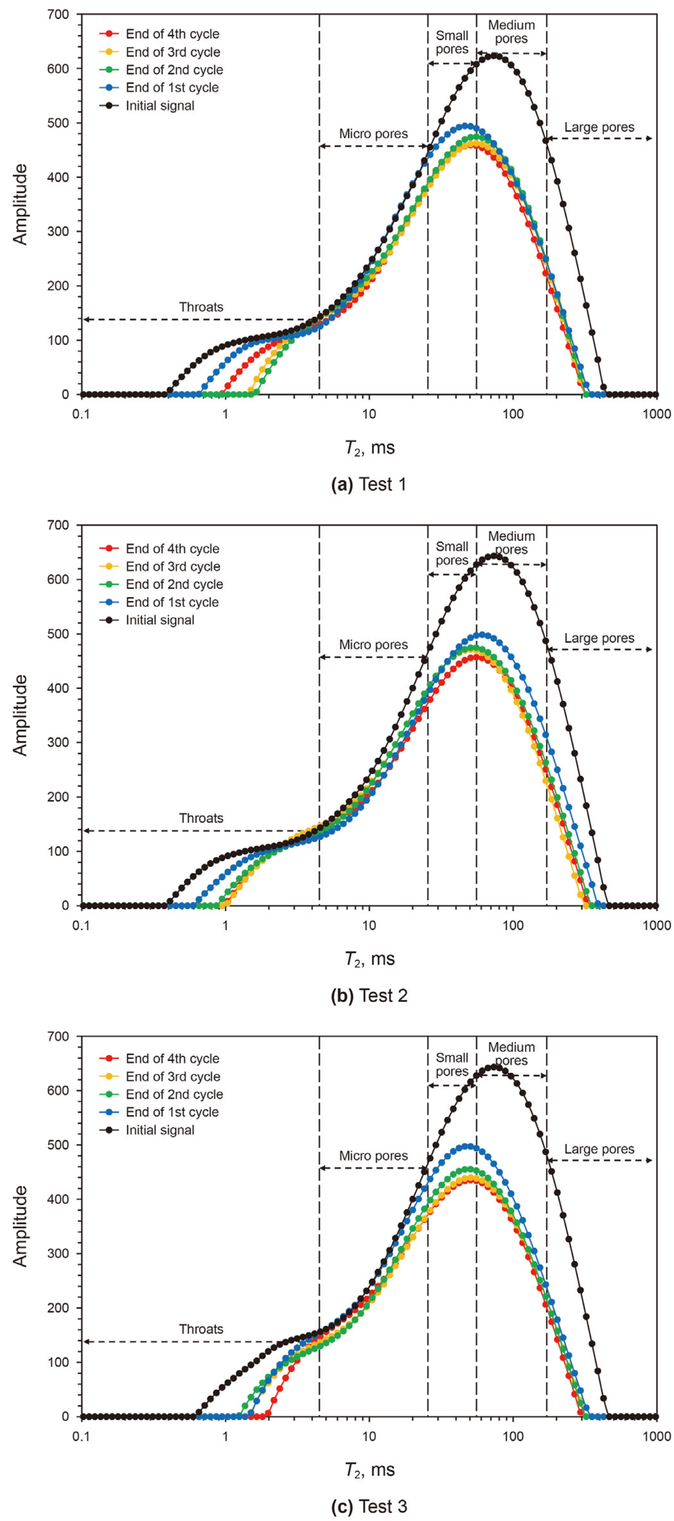

Fig. 4. T_2 spectra under different stages during tests 1, 2 and 3.

core, so the oil recovery factor could be determined by the area difference of the T_2 spectra in different stages. The oil recovery of N_2 HnP is calculated based upon the variation of the T_2 spectra in Fig. 4, and the result is shown in Fig. 5. For test 1, the cumulative oil recovery after 4 cycles is 31.85%. This means that a considerable amount of oil has been produced, which demonstrates the potential of N_2 HnP to enhance the tight oil recovery. The oil recoveries for the first, second, third, and fourth cycles are 23.54%, 6.98%, 1.10%, and 0.23%, respectively. Thus, the first cycle presents the highest oil recovery. The recovery decreased rapidly with the increase in cycle number, and the third and fourth cycles contribute very little to the recovery factor. There are three main reasons for this. First, the oil saturation becomes lower and the continuity of the oil phase becomes worse, which leads to an increase in flow resistance. Second, most of the oil from the high permeability areas has been recovered in the first cycle. Third, the lighter components in the oil are extracted by N_2, causing the remaining oil to become heavier. Therefore, the oil recovered in the subsequent cycles gradually decreases, and two cycles are recommended for N_2 HnP.

The cumulative oil recovery increases slightly from 31.85% to 32.48% when the soaking time is increased from 12 to 24 h. It seems that increasing the soaking time is beneficial to the improvement of oil recovery due to the more adequate contact between N_2 and crude oil. However, the cumulative oil recovery after the second and third cycles at the long soaking time is lower than that at the short soaking time. This is because the oil produced in the second cycle of long soaking time is significantly less than that of short soaking time. Therefore, increasing the soaking time is not necessarily beneficial for N_2 to improve tight oil recovery. The cumulative oil recovery increases significantly from 31.85% to 37.52% when the injection pressure increases by 4 MPa. Besides, the cumulative oil recovery at 28 MPa is higher in all the cycles. Therefore, increasing the injection pressure is beneficial for N_2 to improve tight oil recovery. An important reason is that the solubility of N_2 in the oil increases and the extraction effect is stronger when the pressure of the system is increased, as shown in Table 2. Overall, the oil recovery can be improved by increasing the soaking time and injection pressure, but the injection pressure presents a greater effect than the soaking time; the injection pressure or gas injection volume should be appropriately increased during N_2 HnP for EOR.

Here, a 1D spatial frequency coding sequence is adopted to measure the signal intensity along with different profiles of the core plug under different stages. The shift in signal intensity could represent the change in oil saturation during the development process. Take test 1 as an example (Fig. 6), almost no crude oil can be recovered in the third and fourth cycles, which is in accordance with the conclusion drawn from the T_2 spectrum. In addition, the oil saturation changes at different locations of the core plug are about the same in each cycle, which may imply that a uniform development of N_2 HnP has been achieved along the axial direction. There are two main reasons for this: firstly, the pressure conditions at both ends of the core are identical to amplify the recovery gap between the experimental groups; Secondly, the 1D spatial frequency coding sequence can only capture signals with longer relaxation times, reflecting mainly oil saturation changes in the larger pores.

3.4. EOR Performance in different pores

The oil recovery of different pores under different cycles of test 1 is illustrated in Fig. 7. The recovery in throats isn't discussed here due to the small amount of oil stored in throats. After 4 cycles, the crude oil recovery of 13.26%, 19.23%, 33.11% and 60.51% for micro, small, medium, and large pores, respectively, indicate that the oil from large and medium pores is mainly produced after N_2 HnP. Noted that oil in large pores contributes most to the total recovery in first cycle, however, the oil in micro pores makes the largest contribution to the total recovery in the subsequent cycles. In first cycle, N_2 gas flows mainly via the thief channels, which correspondingly leads to a considerable oil recovery in the large pores. Thereafter, oil from the easily accessible areas has been extracted. In later cycles, N_2 gas enters relatively small and micro pores to

Table 2
Fluid molar composition and properties at 353 K.

Parameter		Dead oil at 24 MPa	With N_2 injection at 24 MPa		With N_2 injection at 28 MPa	
			Oil phase	Gas phase	Oil phase	Gas phase
Molar composition, mol%	N_2	0	33.928	99.859	37.618	99.851
	C_5H_{12}	0.312	0.186	0.021	0.177	0.021
	C_6H_{14}	0.257	0.160	0.010	0.152	0.010
	C_7H_{16}	1.179	0.754	0.027	0.713	0.028
	C_8H_{18}	2.385	1.548	0.032	1.461	0.034
	C_9H_{20}	2.710	1.775	0.020	1.675	0.022
	$C_{10}H_{22}$	3.185	2.096	0.013	1.978	0.014
	$C_{11}H_{24}$	3.252	2.146	0.008	2.026	0.009
	$C_{12}H_{26}$	3.442	2.275	0.004	2.147	0.005
	$C_{13}H_{28}$	3.862	2.555	0.003	2.412	0.003
	$C_{14}H_{30}$	3.659	2.421	0.001	2.286	0.002
	$C_{15}H_{32}$	3.781	2.503	0.001	2.363	0.001
	$C_{16}H_{34}$	2.900	1.920	0.000	1.813	0.000
	$C_{17}H_{36}$	2.426	1.606	0.000	1.516	0.000
	$C_{18}H_{38}$	2.277	1.507	0.000	1.423	0.000
	$C_{19}H_{40}$	2.155	1.427	0.000	1.347	0.000
	C_{20}^{+}	62.217	41.194	0.000	33.133	0.000
Density, kg/m^3		825.464	813.808	213.212	813.71	243.326
Viscosity, mPa s		3.484	3.622	0.028	3.647	0.031

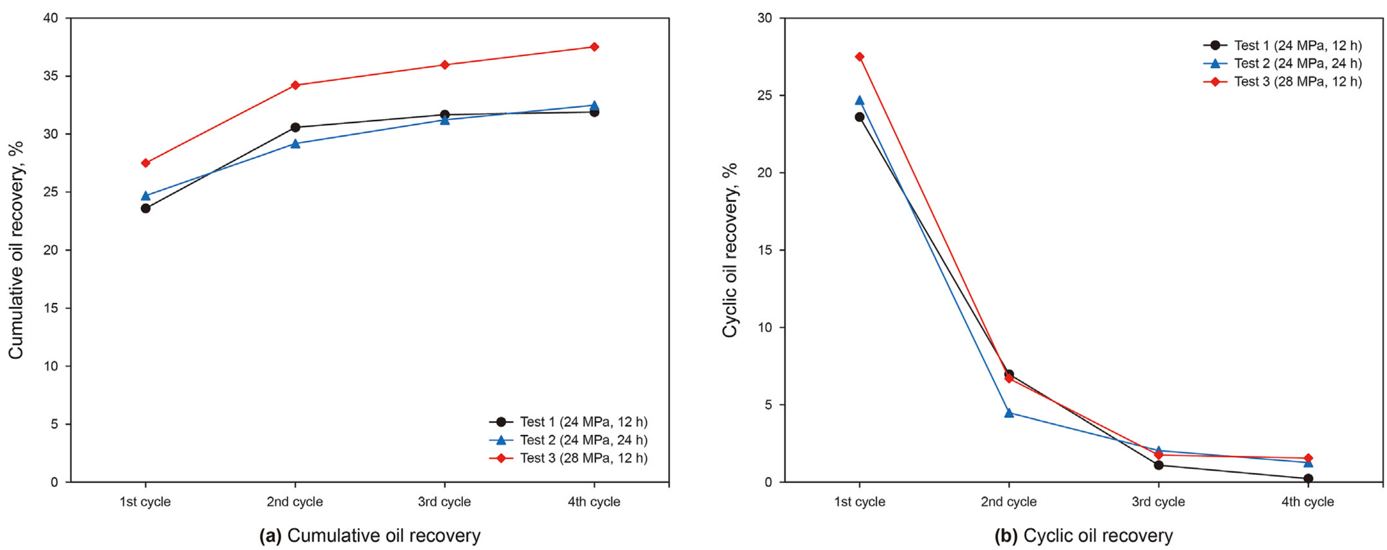

Fig. 5. Cumulative and cyclic oil recovery under different cycles of tests 1, 2, and 3.

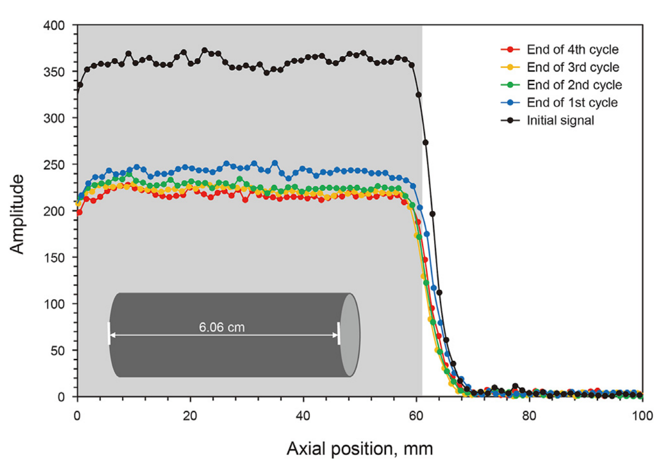

Fig. 6. NMR signal along core plug under different stages of test 1.

extract the hard-to-flow oil. This may also explain why the recovery decreases rapidly with the increasing number of cycles.

Fig. 8 presents the oil recovery of different pores under different cycles for test 2. For the first cycle, the oil recoveries of micro and small pores increase from 2.37% and 11.53% to 15.82% and 18.40%, respectively; however, the oil recoveries of medium and large pores decrease from 29.07% and 54.07% to 25.28% and 40.82%, respectively. In the first cycle, more N_2 enters the smaller pores and the N_2 in the larger pores is relatively reduced as the soak time increases. This results in increased and decreased oil recovery of the smaller and larger pores in the first cycle, respectively. However, the variation in soaking time has a minor effect on the cumulative oil recovery after four cycles for micro, medium, and large pores, with the only slight increase in cumulative oil recovery for the small pores. This indicates that the amount of oil that can be recovered with a given injection of N_2 is stable and does not change significantly with increasing soaking time, and the early production of oil in the micro and small pores increases the difficulty of development in the second cycle. This is the reason why the oil recovery in

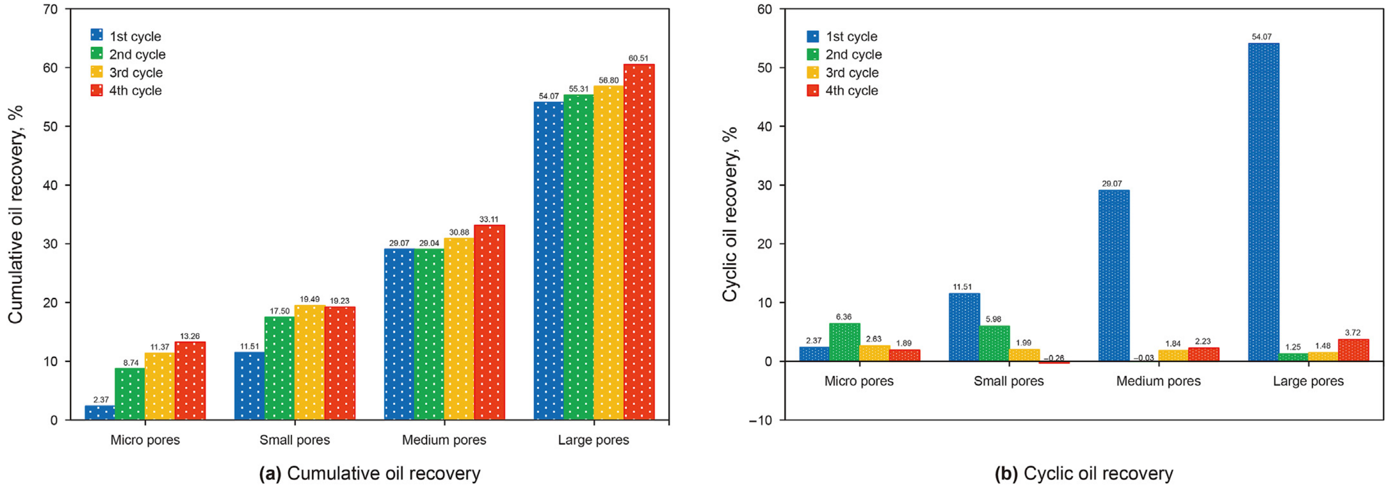

Fig. 7. Oil recovery of different pores for test 1.

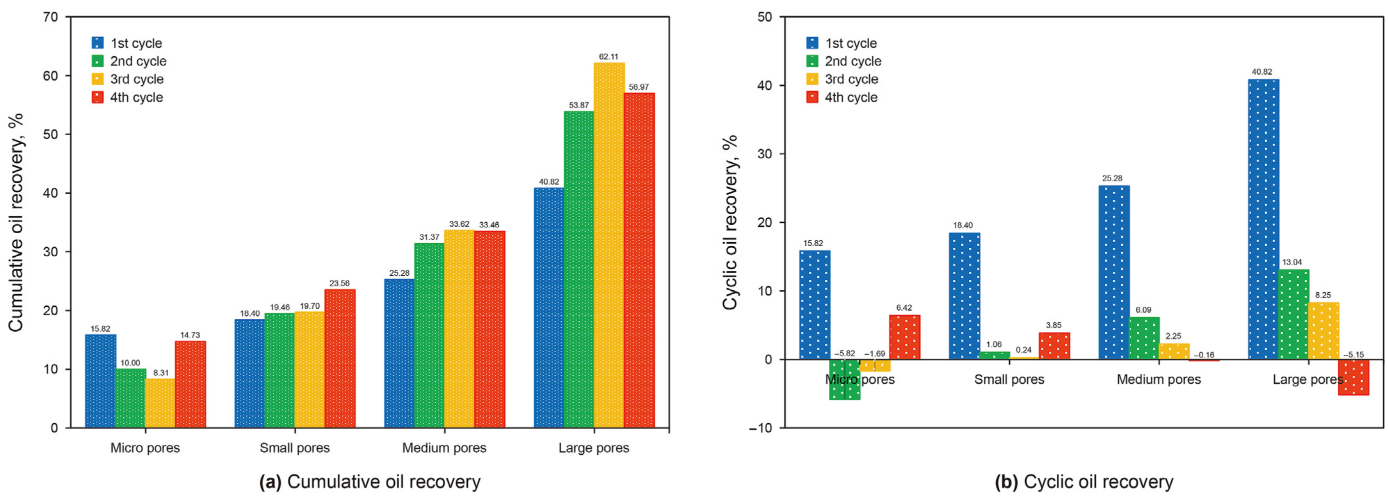

Fig. 8. Oil recovery of different pores for test 2.

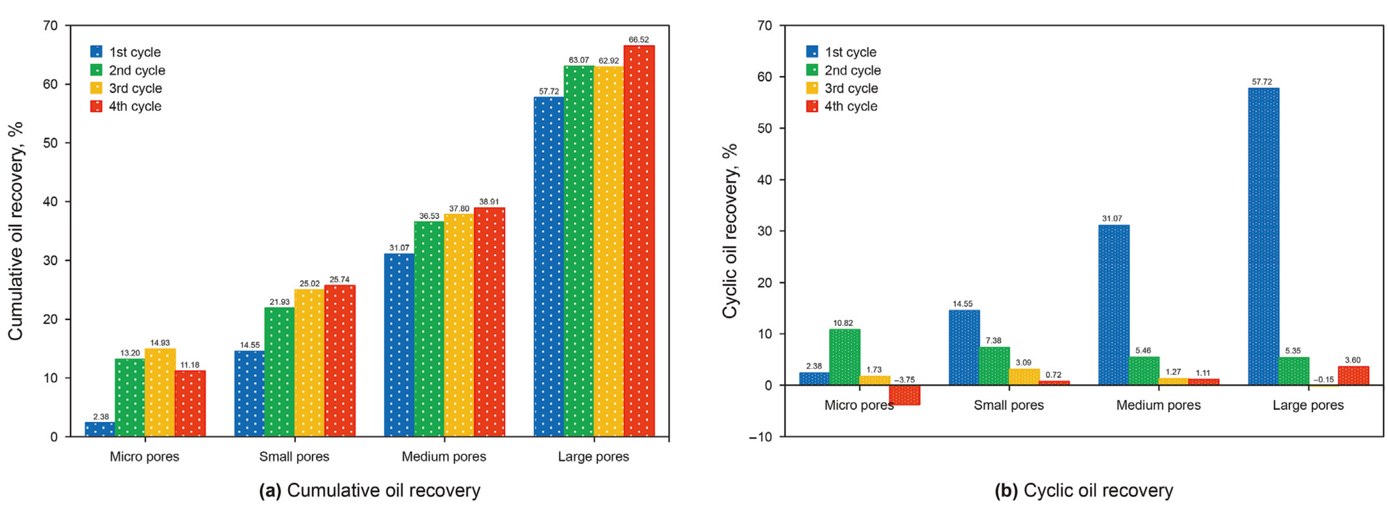

Fig. 9. Oil recovery of different pores for test 3.

the second cycle decreases when the soaking time increases.

The cumulative and cyclic oil recovery of different pores under different cycles for test 3 is given in Fig. 9. The results show that after increasing the injection pressure by 4 MPa, the cumulative oil recoveries of small, medium, and large pores are all significantly improved. The difference is that the recovery factor is increased for each cycle in small pores, increased for the first and second cycles and slightly decreased for the third and fourth cycles in the medium and large pores. Interestingly, increasing the injection pressure presents no obvious effect on the oil recovery of micro pores. For instance, the oil recovery in the third cycle increases slightly from 11.37% to 14.93%, while the oil recovery in the fourth cycle decreases slightly from 13.26% to 11.18%. This is because the increased pressure makes it easier for gas to flow along the high permeability channel. In this case, the N_2 gas is mainly stored in the larger pores. Although the amount of injected N_2 has increased, the N_2 in the micro pores may not increase. Therefore, increasing the injection pressure results in a significant increase in the oil recovery factor of the large, medium, and small pores, but present no apparent effect on the recovery factor of the micro pores.

4. Conclusions

In this work, a non-magnetic reactor, with a maximum temperature resistance of 393.15 K and pressure resistance of 40 MPa, was developed and combined with NMR equipment for N_2 HnP experiments. The EOR performance and governing factor of N_2 HnP in specific pores were analyzed at different cycle numbers, soaking times, and injection pressures. The main findings and conclusions of this paper can be drawn:

(1) The cumulative oil recovery after four cycles can reach 37.52%, which demonstrates the potential of N_2 HnP to recover tight oil. The first cycle presents the highest oil recovery. The oil recovery decreases rapidly with the increase in cycle number, and the third and fourth cycles contribute very little to the recovery factor. Two cycles are recommended for N_2 HnP.
(2) The pore space is uniformly subdivided into four parts according to pore size and amount of saturated oil: micro, small, medium, and large pores. The highest recoveries after N_2 HnP are obtained in the large pores (57%–67%), followed by the medium pores (33%–39%), the small pores (19%–26%) and finally the micro pores (11%–15%).
(3) Increasing the soaking time (10 h → 20 h) slightly improves the oil recovery (0.63%), and the effectiveness is mainly reflected in the first cycle. An increase in soaking time can improve the oil recoveries of the micro and small pores and reduce the oil recoveries of the medium and large pores in the first cycle. However, the change in soaking time had no significant effect on the cumulative oil recoveries after four cycles in micro, medium, and large pores, with only a slight increase in cumulative oil recovery in the small pores.
(4) Increasing the injection pressure (24 MPa → 28 MPa) significantly increases the oil recovery (5.67%), and the effectiveness is mainly seen in the first cycle. An increase in injection pressure can increase the oil recoveries of small, medium, and large pores, but presents no obvious effect on the recovery factor of micro pores.
(5) NMR T_2 spectra and flash calculation results indicate dissolution and extraction effects are important for N_2 HnP EOR.

Acknowledgments

We acknowledge the financial support from the National Natural Science Foundation of China (52074319), the Strategic Cooperation Technology Project of CNPC (ZLZX2020-01-08), and the Science Foundation of China University of Petroleum-Beijing (2462021QNXZ008).

References

Altawati, F., Emadi, H., Pathak, S., 2021. Improving oil recovery of Eagle Ford shale samples using cryogenic and cyclic gas injection methods - an experimental study. Fuel 302, 121170. https://doi.org/10.1016/j.fuel.2021.121170.
Bai, H., Zhang, Q., Li, Z., Li, B., Zhu, D., Zhang, L., Lv, G., 2019. Effect of fracture on production characteristics and oil distribution during CO_2 huff-n-puff under tight and low-permeability conditions. Fuel 246, 117–125. https://doi.org/10.1016/j.fuel.2019.02.107.
Burrows, L.C., Haeri, F., Cvetic, P., Sanguinito, S., Shi, F., Tapriyal, D., Goodman, A., Enick, R.M., 2020. A literature review of CO_2, natural gas, and water-based fluids for enhanced oil recovery in unconventional reservoirs. Energy Fuel. 34 (5), 5331–5380. https://doi.org/10.1021/acs.energyfuels.9b03658.
Chen, M., Dai, J., Liu, X., Kuang, Y., Qin, M., Wang, Z., 2019. Contributions of pore-throat size distribution to reservoir quality and fluid distribution from NMR and MIP in tight sandy conglomerate reservoirs. Arabian J. Geosci. 12 (1), 1–12. https://doi.org/10.1007/s12517-018-4153-7.
Dong, X., Shen, L.W., Golsanami, N., Liu, X., Sun, Y., Wang, F., Shi, Y., Sun, J., 2020a. How N_2 injection improves the hydrocarbon recovery of CO_2 HnP: an NMR study on the fluid displacement mechanisms. Fuel 278, 118286. https://doi.org/10.1016/j.fuel.2020.118286.
Dong, X., Shen, L.W., Liu, X., Zhang, P., Sun, Y., Yan, W., Jiang, L., Wang, F., Sun, J., 2020b. NMR characterization of a tight sand's pore structures and fluid mobility: an experimental investigation for CO_2 EOR potential. Mar. Petrol. Geol. 118, 104460. https://doi.org/10.1016/j.marpetgeo.2020.104460.
Du, D., Pu, W., Jin, F., Liu, R., 2020. Experimental study on EOR by CO_2 huff-n-puff and CO_2 flooding in tight conglomerate reservoirs with pore scale. Chem. Eng. Res. Des. 156, 425–432. https://doi.org/10.1016/j.cherd.2020.02.018.
Feng, Q., Xu, S., Xing, I., Zhang, W., Wang, S., 2020. Advances and challenges in shale oil development: a critical review. Adv. Geo-Energy Res. 4 (4), 406–418. https://doi.org/10.46690/ager.2020.04.06.
Hamdi, H., Clarkson, C.R., Ghanizadeh, A., Ghaderi1, S.M., Vahedian1, A., Riazi1, N., Esmail, A., 2018. Huff-n-puff gas injection performance in shale reservoirs: a case study from Duvernay Shale in Alberta, Canada. In: Unconventional Resources Technology Conference. https://doi.org/10.15530/urtec-2018-2902835.
Huang, H., Li, R., Xiong, F., Hu, H., Sun, W., Jiang, Z., Chen, L., Wu, L., 2020. A method to probe the pore-throat structure of tight reservoirs based on low-field NMR: insights from a cylindrical pore model. Mar. Petrol. Geol. 117, 104344. https://doi.org/10.1016/j.marpetgeo.2020.104344.
Huang, X., Li, A., Li, X., Liu, Y., 2019. Influence of typical core minerals on tight oil recovery during CO_2 flooding using the nuclear magnetic resonance technique. Energy Fuel. 33 (8), 7147–7154. https://doi.org/10.1021/acs.energyfuels.9b01220.
Jia, H., Liu, P., Pu, W., Ma, X., Zhang, J., Gan, L., 2016. In situ catalytic upgrading of heavy crude oil through low-temperature oxidation. Petrol. Sci. 13 (3), 476–488. https://doi.org/10.1007/s12182-016-0113-6.
Kewen, W., Ning, L., 2008. Numerical simulation of rock pore-throat structure effects on NMR T_2 distribution. Appl. Geophys. 5 (2), 86–91. https://doi.org/10.1007/s11770-008-0013-7.
Li, L., Sheng, J.J., Su, Y., Zhan, S., 2018. Further investigation of effects of injection pressure and imbibition water on CO_2 huff-n-puff performance in liquid-rich shale reservoirs. Energy Fuel. 32 (5), 5789–5798. https://doi.org/10.1021/acs.energyfuels.8b00536.
Li, S., Wang, Q., Zhang, K., Li, Z., 2020. Monitoring of CO_2 and CO_2 oil-based foam flooding processes in fractured low-permeability cores using nuclear magnetic resonance (NMR). Fuel 263, 116648. https://doi.org/10.1016/j.fuel.2019.116648.
Lu, T., Li, Z., Li, J., Hou, D., Zhang, D., 2017. Flow behavior of N_2 huff and puff process for enhanced oil recovery in tight oil reservoirs. Sci. Rep.-UK 7 (1). https://doi.org/10.1038/s41598-017-15913-5.
Ma, Q., Yang, S., Lv, D., Wang, M., Chen, J., Kou, G., Yang, L., 2019. Experimental investigation on the influence factors and oil production distribution in different pore sizes during CO_2 huff-n-puff in an ultra-high-pressure tight oil reservoir. J. Petrol. Sci. Eng. 178, 1155–1163. https://doi.org/10.1016/j.petrol.2019.04.012.
Mahzari, P., Mitchell, T.M., Jones, A.P., Oelkers, E.H., Striolo, A., Iacoviello, F., Shearing, P.R., Ernesto Juri, J., 2021. Novel laboratory investigation of huff-n-puff gas injection for shale oils under realistic reservoir conditions. Fuel 284, 118950. https://doi.org/10.1016/j.fuel.2020.118950.
Nguyen, P., Carey, J.W., Viswanathan, H.S., Porter, M., 2018. Effectiveness of supercritical-CO_2 and N_2 huff-and-puff methods of enhanced oil recovery in shale fracture networks using microfluidic experiments. Appl. Energy 230, 160–174. https://doi.org/10.1016/j.apenergy.2018.08.098.
Qian, K., Yang, S., Dou, H., Wang, Q., Wang, L., Huang, Y., 2018. Experimental investigation on microscopic residual oil distribution during CO_2 huff-and-puff process in tight oil reservoirs. Energies 11 (10), 2843. https://doi.org/10.3390/en11102843.
Sheng, J.J., Mody, F., Griffith, P.J., Barnes, W.N., 2016. Potential to increase condensate oil production by huff-n-puff gas injection in a shale condensate reservoir.

J. Nat. Gas Sci. Eng. 28, 46–51. https://doi.org/10.1016/j.jngse.2015.11.031.
Song, Y., Gu, S., Song, Z., Zhang, Z., Chang, X., Guo, J., 2022a. Effect of confinement on the three-phase equilibrium of water-oil-CO_2 mixtures in nanopores. Petrol. Sci. 19 (1), 203–210. https://doi.org/10.1016/j.petsci.2021.09.024.
Song, Y., Song, Z., Guo, J., Feng, D., Chang, X., 2021a. Phase behavior and miscibility of CO_2–hydrocarbon mixtures in shale nanopores. Ind. Eng. Chem. Res. 60 (14), 5300–5309. https://doi.org/10.1021/acs.iecr.1c00717.
Song, Y., Song, Z., Zeng, H., Tai, C., Chang, X., 2022b. N_2 and CO_2 huff-n-puff for enhanced tight oil recovery: an experimental study using nuclear magnetic resonance. Energy Fuel. 36 (3), 1515–1521. https://doi.org/10.1021/acs.energyfuels.1c03982.
Song, Z., Song, Y., Guo, J., Feng, D., Dong, J., 2021b. Effect of nanopore confinement on fluid phase behavior and production performance in shale oil reservoir. Ind. Eng. Chem. Res. 60 (3), 1463–1472. https://doi.org/10.1021/acs.iecr.0c05814.
Song, Z., Song, Y., Li, Y., Bai, B., Song, K., Hou, J., 2020. A critical review of CO_2 enhanced oil recovery in tight oil reservoirs of North America and China. Fuel 276, 118006. https://doi.org/10.1016/j.fuel.2020.118006.
Sun, R., Yu, W., Xu, F., Pu, H., Miao, J., 2019. Compositional simulation of CO_2 huff-n-puff process in Middle Bakken tight oil reservoirs with hydraulic fractures. Fuel 236, 1446–1457. https://doi.org/10.1016/j.fuel.2018.09.113.
Wan, T., Liu, H., 2018. Exploitation of fractured shale oil resources by cyclic CO_2 injection. Petrol. Sci. 15 (3), 552–563. https://doi.org/10.1007/s12182-018-0226-1.
Wan, T., Wang, W., Jiang, J., Zhang, Y., 2018. Pore-scale analysis of gas huff-n-puff enhanced oil recovery and waterflooding process. Fuel 215, 561–571. https://doi.org/10.1016/j.fuel.2017.11.033.
Wang, M., Chen, S., Lin, M., 2018. Enhancing recovery and sensitivity studies in an unconventional tight gas condensate reservoir. Petrol. Sci. 15 (2), 305–318. https://doi.org/10.1007/s12182-018-0220-7.
Wei, B., Gao, K., Song, T., Zhang, X., 2020. Nuclear-magnetic-resonance monitoring of mass exchange in a low-permeability matrix/fracture model during CO_2 cyclic injection: a Mechanistic Study. SPE J. 25 (1), 440–450. https://doi.org/10.2118/199345-PA.
Xiao, D., Jiang, S., Thul, D., Huang, W., Lu, Z., Lu, S., 2017. Combining rate-controlled porosimetry and NMR to probe full-range pore throat structures and their evolution features in tight sands: a case study in the Songliao Basin, China. Mar. Petrol. Geol. 83, 111–123. https://doi.org/10.1016/j.marpetgeo.2017.03.003.
Yu, W., Lashgari, H.R., Wu, K., Sepehrnoori, K., 2015. CO_2 injection for enhanced oil recovery in Bakken tight oil reservoirs. Fuel 159, 354–363. https://doi.org/10.1016/j.fuel.2015.06.092.
Yu, Y., Li, L., Sheng, J.J., 2017. A comparative experimental study of gas injection in shale plugs by flooding and huff-n-puff processes. J. Nat. Gas Sci. Eng. 38, 195–202. https://doi.org/10.1016/j.jngse.2016.12.040.
Yue, P., Xie, Z., Huang, S., Liu, H., Liang, S., Chen, X., 2018. The application of N_2 huff and puff for IOR in fracture-vuggy carbonate reservoir. Fuel 234, 1507–1517. https://doi.org/10.1016/j.fuel.2018.07.128.
Zhang, Y., Yu, W., Li, Z., Sepehrnoori, K., 2018. Simulation study of factors affecting CO_2 huff-n-puff process in tight oil reservoirs. J. Petrol. Sci. Eng. 163, 264–269. https://doi.org/10.1016/j.petrol.2017.12.075.
Zhu, C., Guo, W., Wang, Y., Li, Y., Gong, H., Xu, L., Dong, M., 2020. Experimental study of enhanced oil recovery by CO_2 huff-n-puff in shales and tight sandstones with fractures. Petrol. Sci. https://doi.org/10.1007/s12182-020-00538-7.
Zuloaga, P., Yu, W., Miao, J., Sepehrnoori, K., 2017. Performance evaluation of CO_2 huff-n-puff and continuous CO_2 injection in tight oil reservoirs. Energy 134, 181–192. https://doi.org/10.1016/j.energy.2017.06.028.